Hydrothermal doping of nitrogen in bamboo-based super activated carbon for hydrogen storag

Luo, L., Chen, T., Zhao, W., and Fan, M. (2017). **"Hydrothermal doping of nitrogen in bamboo-based super activated carbon for hydrogen storage,"** *BioRes.* 12(3), 6237-6250.

Abstract

N-doped microporous activated carbons were synthesized by hydrothermal doping with ammonia as the nitrogen precursor; the chemical, structural, and hydrogen storage properties of the developed activated carbons (ACs) were also examined. The results showed that this method is an effective way of preparing microporous activated carbons with high surface area. Both the surface areas and the N contents of ACs were increased after hydrothermal doping, and hence, the hydrogen storage capacities were improved. The hydrogen storage capacity of the N-doped ACs was 3.10 wt.% at 77 K and 1 bar, showing an enhancement factor of 1.13 and corresponding to the NAC with both highest surface area (3485 m^2/g) and N content (2.2 wt.%). Statistical analysis showed that both the N content and surface area had positive contributions to the hydrogen storage, and it also could be predicted by the linear model from the N content and surface area. These results were among the best in hydrogen storage carbon materials, and the high hydrogen storage capacities were attributed to the high surface area.

Download PDF → (https://bioresources.cnr.ncsu.edu/wp-content/uploads/2017/07/BioRes_12_3_6237_Luo_CZF_Hydrothermal_Doping_Bamboo_based_Activ_

Full Article

Hydrothermal Doping of Nitrogen in Bamboo-Based Super Activated Carbon for Hydrogen Storage

Lu Luo,[a] Tingting Chen,[a] Weigang Zhao,[a,*] and Mizi Fan [a,b]

N-doped microporous activated carbons were synthesized by hydrothermal doping with ammonia as the nitrogen precursor; the chemical, structural, and hydrogen storage properties of the developed activated carbons (ACs) were also examined. The results showed that this method is an effective way of preparing microporous activated carbons with high surface area. Both the surface areas and the N contents of ACs were increased after hydrothermal doping, and hence, the hydrogen storage capacities were improved. The hydrogen storage capacity of the N-doped ACs was 3.10 wt.% at 77 K and 1 bar, showing an enhancement factor of 1.13 and corresponding to the NAC with both highest surface area (3485 m^2/g) and N content (2.2 wt.%). Statistical analysis showed that both the N content and surface area had positive contributions to the hydrogen storage, and it also could be predicted by the linear model from the N content and surface area. These results were among the best in hydrogen storage carbon materials, and the high hydrogen storage capacities were attributed to the high surface area.

Keywords: Nitrogen doping; Activated carbon; Hydrogen adsorption; Hydrothermal

Contact information: a: College of Material Engineering, Fujian Agriculture and Forestry University, NO 63 Xiyuangong Road, Fuzhou 350002, PR China; b: College of Engineering Design and Physical Sciences, Brunel University, Uxbridge UB8 3PH, United Kingdom;

** Corresponding author: weigang-zhao@hotmail.com*

INTRODUCTION

As a highly efficient and clean energy, hydrogen has great potential to be further exploited. It can be used as fuel for cars, light trucks, ships, airplanes, and trains and to generate electricity for heating and manufacturing (Zhao *et al.* 2013; Wróbel-Iwaniec *et al.* 2015). However, the greatest problem associated with hydrogen is the storage method. The US Department of Energy (DOE) set the goals in 2009 for hydrogen storage systems, which are reversibility, gravimetric density around 6 wt.% (Zhao *et al.* 2013), and heat of adsorption within the 20 kJ/mol to 30 kJ/mol range (Zhao *et al.* 2005). Activated carbons (ACs) were considered for hydrogen storage due to the advantage of reversibility, high specific surface area, porous microstructure, and stability for large scale production (Xie *et al.* 2013; Hwang *et al.* 2015; Zhao *et al.* 2016).

However, unsubstituted carbon-based materials only bind one hydrogen molecule on each side of a carbon ring with the binding energy of 4 kJ/mol to 5 kJ/mol, which is much lower than the ideal adsorption range (20 kJ/mol to 30 kJ/mol) (Hubner *et al.* 2004). To improve hydrogen storage, the gas-solid interaction can be strengthened by introducing metal nanoparticles (Pd, Ni, Pt) or heteroatoms (B, N, S, P) in the carbon matrix (Fu *et al.* 2012; Zhao *et al.* 2013; Adhikari *et al.* 2016; Wang *et al.* 2016). Nitrogen doping has been studied extensively, and various theoretical investigations show that the doping of nitrogen atoms increases the adsorption energy of hydrogen atoms at the neighboring C-atom sites (Zheng *et al.* 2010; Xia *et al.* 2011; Fu *et al.* 2012; Zhao *et al.* 2013; Huang *et al.* 2015).

The hydrogen storage of ACs at 77 K primarily depends on the surface area and microporosity. N doping may decrease the micropore volume and surface area available for adsorption, leading to decreased hydrogen storage capacity (Xia *et al.* 2011; Zhao *et al.* 2013). Therefore, to achieve a real improvement in hydrogen storage by nitrogen doping, other key parameters, especially the surface area and microporosity, must be unchanged or enhanced. Currently, there is no report about N-doped ACs synthesized by the hydrothermal method from bamboo for hydrogen storage.

In this study, nitrogen doped high surface area ACs were synthesized with hydrothermal treatment, using ammonia as a nitrogen source. The chemical, structural, and hydrogen storage properties of the developed ACs were examined. The results provide an effective method for heteroatom doping and offer a potentially cost-effective alternative to the commercial use of ACs for hydrogen storage. These findings also provide further evidence that N doping has a positive contribution to hydrogen storage.

EXPERIMENTAL

Materials

Potassium hydroxide (KOH), ammonia (28%), and hydrochloric acid (HCl) were purchased from Tianjin Fuchen Chemical Reagents Factory (Tianjin, China). All were analytic grade and used without further purification or treatment.

Preparation of the Activated Carbon from Bamboo

Moso bamboo (*Phyllostachys edulis)* from Fujian Province (China) was selected as the char precursor. AC was prepared through carbonization and then KOH activation, as described previously (Zhao *et al.* 2016). Bamboo char (BC) prepared from the bamboo culms was obtained in a horizontal tubular furnace under a pure nitrogen environment (flow rate, 300 mL/min) at 650 °C with gradually increased temperature (5 °C /min). The BC was further ground and sieved with an average size of 100 μm to 200 μm.

For the activation, bamboo char powder was mixed with KOH with weight ratios ($W = 4$, which means that the weight ratio of KOH/bamboo char is 4), and placed in a nickel crucible. A muffle furnace (80-plus, KDF, Japan) was used for heat treatment under a stream of nitrogen (300 mL/min) with constant heating rate (3 °C /min) up to the final activation temperature 800 °C and kept for 2 h. After cooling to room temperature under nitrogen flow, the activated carbon was washed first with 1 M HCl, followed with 250 mL soxhlet extraction until it reached a constant pH. Finally, the AC was oven-dried for 24 h to obtain the very pure activated carbon (AC) material. The developed AC was stored for the subsequent hydrothermal treatment.

Preparation of N-Doped ACs

First, 500 mg of prepared AC was mixed with 36 g of 28% ammonia solution and 12 g of ethylene glycol solution, and the mixture was sonicated for 30 min. The resulting mixture was transferred into a sealed Teflon autoclave. The synthesis temperature was fixed at 180 °C for 3, 6, 12, or 24 h. The mixtures were then filtered and washed for 3 days with 250 mL soxhlet extraction and then oven-dried at 80 °C for 12 h. The four N-doped ACs were designated as NAC1 (3 h), NAC2 (6 h), NAC3 (12 h), and NAC4 (24 h).

Characterization of the ACs: Nitrogen Content Determination

The morphologies and scanning electron microscopy with energy dispersive X-ray (SEM-EDX) were carried out using scanning transmission electron microscopy (SEM; FEG SEM, Hitachi S 3400, Tokyo, Japan) and high resolution transmission electronic microscopy (HRTEM, JEOL JEM-2100, Tokyo, Japan; accelerating voltage of 200 kV). The elemental analysis (EA) was determined by an Elementar Vario EL (Elementar Analysensysteme, Germany) and by an X-ray photoelectron spectrometer (XPS; SPECS XPS system, Berlin, Germany) using 150 W Al-Kα radiation.

Nitrogen Physisorption and Hydrogen Storage Performance

The nitrogen and hydrogen adsorption data were obtained and treated as described elsewhere (Zhao *et al.* 2011; Wróbel-Iwaniec *et al.* 2015; Zhao *et al.* 2016). A Micrometrics ASAP 2020 automatic apparatus (Micromeritics, Co., USA) was used to obtain the N_2 and hydrogen isotherms.

Before adsorption analysis, the samples were degassed for 24 h under vacuum at 393 K. The N_2 adsorption data were processed to generate: (i) surface area, S_{BET}, by the BET calculation method (Brunauer *et al.* 1938); (ii) micropore volume, V_{DR}, according to the Dubinin-Radushkevich (DR) method (Dubinin and Polstyanov 1989); and (iii) total pore volume, $V_{0.99}$, defined as the volume of liquid nitrogen corresponding to the amount adsorbed at a relative pressure P/P_0 = 0.99 (Gregg and Sing 1982). The average micropore diameter, L_0, (Stoeckli *et al.* 2002) and the pore size distributions (PSD) by application of the Density Functional Theory (DFT) (Tarazona 1995) were also calculated. EA is the characteristic adsorption energy of nitrogen and was derived from the corresponding adsorption isotherms at 77 K, applying the DR method (Dubinin and Polstyanov 1989). The H_2 adsorption capacities were obtained from the H_2 adsorption isotherms at 77 K up to 1 bar.

Statistical Analysis

The statistical analysis was performed with SPSS 18.0 software (IBM SPSS Statistics. Co., Armonk, NY, USA). The N content and surface area were set as two independent variables, and the hydrogen storage was set as dependent variable. The regression analysis was used to study the contribution of N content and surface area to the H_2 uptake.

RESULTS AND DISCUSSION

AC Characterization

The elemental analysis results showed that the C contents were 46.12 wt.%, 77.10 wt.%, and 90.11 wt.% for bamboo, BC, and AC, respectively. The nitrogen contents of bamboo, BC, and AC were all very low, about 0.3 wt.%, whereas the content of the N-doped ACs was between 0.80 wt.% and 1.86 wt.%.

Figure 1 shows the effect of hydrothermal doping time on the nitrogen content, as determined by the elemental analysis; the N content linearly increased with extended hydrothermal doping time.

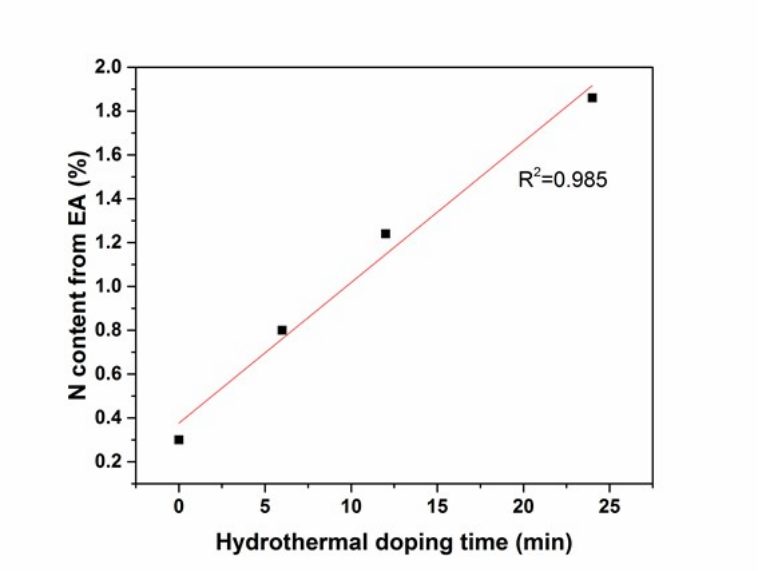

Fig. 1. The N content with different hydrothermal doping time

XPS Studies

XPS analysis was used to investigate the element composition and chemical status of sample NAC3, as shown in Fig. 2a. The nitrogen contents of AC and NAC3 were 0.5 wt.% and 2.2 wt.%, respectively, which was in agreement with the elemental analysis results. This demonstrated that the hydrothermal treatment was an effective way for the synthesis of N-doped microporous ACs. Figures 2b and 2c show the regions corresponding to C1s and N1s from the high resolution XPS. The N1s spectrum was assigned into three N species, which were pyridinic-N at 398.7 eV, pyrrolic-N at 399.9 eV, and quaternary-N at 401.0 eV, confirming three types of N species in the carbon framework (Fan *et al.* 2014; Sari and Ting 2015). The C1s spectrum displayed an asymmetric shape, with the four components of carbon species corresponding to C-C/C=C at 284.6 eV, C-OH/C-O-C at 285.3 eV, C=O/C-N at 286.2 eV, and C(O)OH/C(O)-O-C at 288.5

eV in NAC3, which further confirmed that the N was doped into the AC (Fan *et al.* 2014; Sari and Ting 2015). The N content of NAC3 with different hydrothermal doping time measured by the XPS (not shown) and EA were both increased in a nearly linear fashion. In summary, N atoms were successfully doped in ACs by the hydrothermal process.

SEM Analysis

SEM micrographs of NAC samples are shown in Fig. 3a. Abundant pores and pristine vascular bundle structure were retained from the raw bamboo, which were favorable for the diffusion of H_2. It was also speculated that a large number of invisible micropores and macropores should exist due to the high surface area determined by the N_2 adsorption-desorption analysis, but they were not visible on this SEM image. The HRTEM images displayed in Fig. 3f further illustrated the amorphous and microporous structure of N-doped sample.

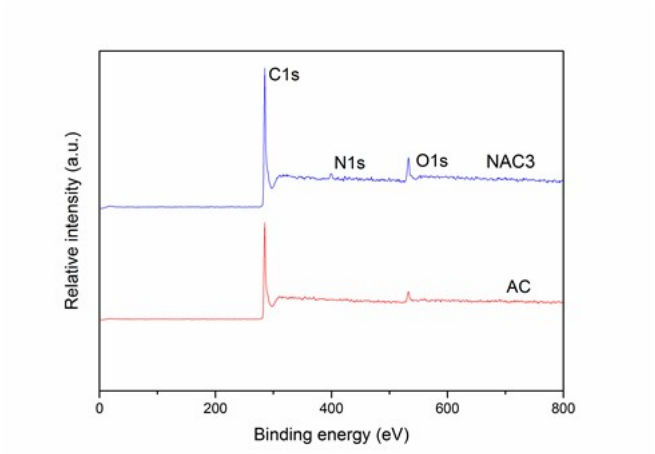

(a)

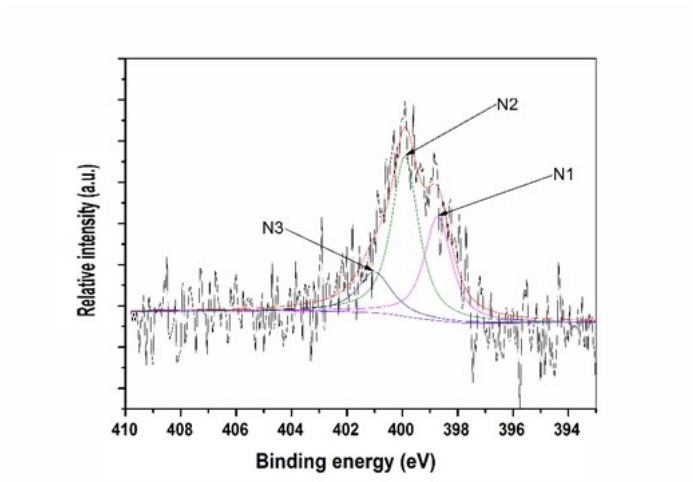

(b)

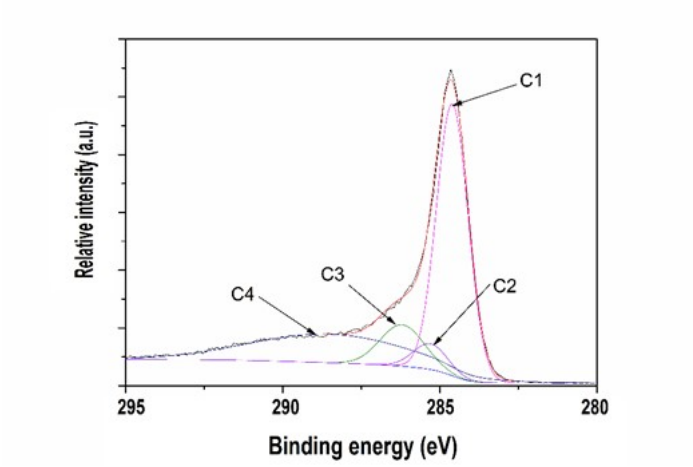

(c)

Fig. 2. XPS spectra (a) and deconvoluted high-resolution of N1s (b), C1s (c) of NAC3

The corresponding EDX elemental mappings from SEM and TEM are depicted in Fig. 3b to 3e. Notably, the distribution of the different heteroatoms (oxygen and nitrogen) in the N-doped AC was quite uniform. This indicated that the hydrothermal doping treatment was effective uniformly reacted on the entire surface.

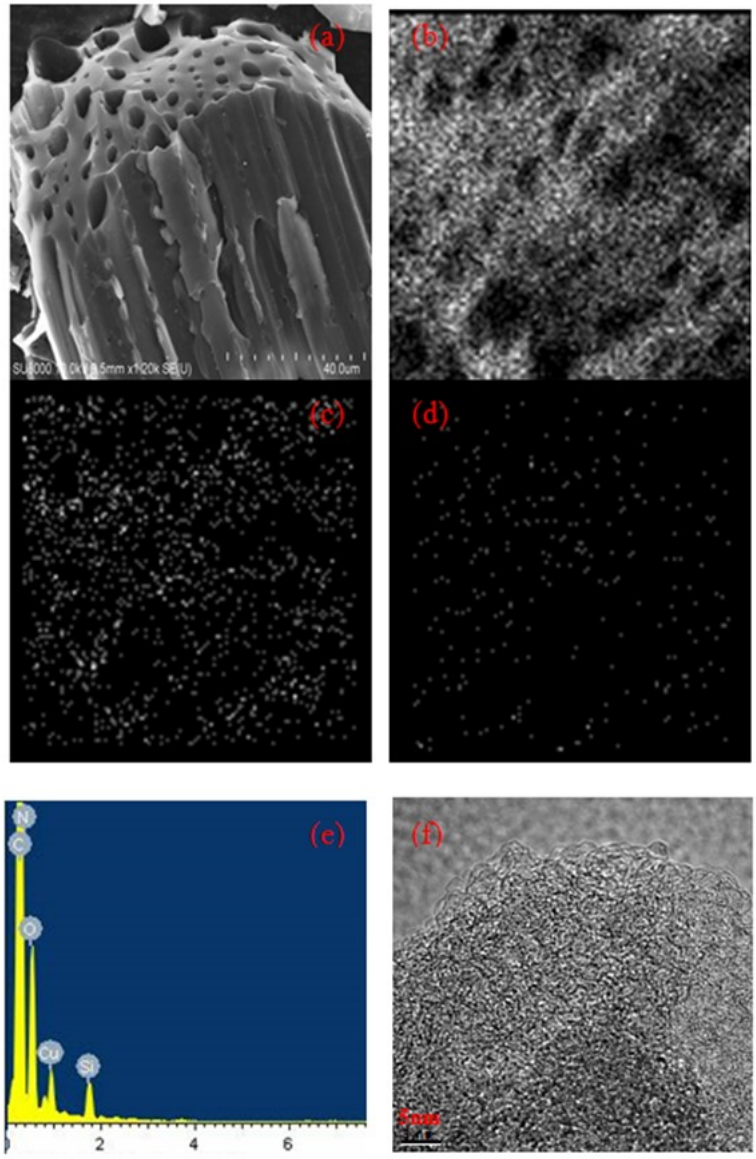

Fig. 3. SEM images of NAC sample (a) and EDX mapping of NAC sample for C (b), O (c), and N (d); EDX analyses of NAC sample (e); TEM image of NAC sample (f)

Porous Texture

Table 1 shows the textural parameters of the bamboo char, activated carbon, and nitrogen doped activated carbons determined by N_2 adsorption at 77 K. The surface area of bamboo char was only 337 m^2/g. After KOH activation and hydrothermal treatment, the surface areas of all the ACs were higher than 3000 m^2/g, *i.e.*, between 3262 m^2/g and 3485 m^2/g, which were among the highest reported in the literature (Xie *et al.* 2013; Hwang *et al.* 2015; Zhao *et al.* 2016). Both the AC and the nitrogen doped ACs were mainly classified as microporous due to the $V_{DR}/V_{0.99}$, which ranged from 0.64 cm^3/g to 0.65 cm^3/g. These carbons also had large mesopores. After the hydrothermal N doping, both the surface area and pore volume were increased, as observed in the pore size ranges. This finding agreed with the results of Pietrzak *et al.* (2006). This is because the pore structures of the NACs not only produced from the KOH activation, but also the hydrothermal process. With the high pressure and temperature in hydrothermal process, some new pores were produced and the pores could also penetrate to each other. The hydrogen storage capacities were linearly increased with the surface area and micropore volume, indicating that the hydrothermal doping treatment in this study was an effective way to improve the hydrogen storage.

Table 1. Textural Characterization of all the ACs

Samples	S_{BET} (m^2/g)	$V_{0.99}$ (cm^3/g)	V_{DR} (cm^3/g)	EA (kJ/mol)	L_0 (nm)	$V_{DR}/V_{0.99}$ (cm^3/g)	V_{meso} (cm^3/g)
BC	337	0.14	N	N	N	N	N
AC	3262	1.56	1.01	19.07	1.41	0.65	0.55
NAC1	3301	1.60	1.02	19.15	1.39	0.64	0.58
NAC2	3394	1.64	1.05	19.18	1.39	0.64	0.59
NAC3	3485	1.67	1.07	19.16	1.39	0.64	0.60

Figure 4a shows N_2 adsorption-desorption isotherms of all the AC and NAC samples at 77 K. It was apparent that all the isotherms were type I according to the IUPAC classification, indicating the presence of microporosity and some mesoporosity (with a size between 2 nm and 4 nm). Thus, hydrothermal treatment had no effect on the isotherm shape but did affect all pore volumes. Interestingly, the S_{BET} (3301 m^2/g, 3394 m^2/g, and 3485 m^2/g) was increased with the hydrothermal time, which is favorable for hydrogen storage (Fu *et al.* 2012; Zhao *et al.* 2013). The pore size distributions of N_2 adsorption isotherms are represented in Fig. 4b, which confirmed that all samples were mainly microporous. After the hydrothermal treatment, all pore volumes were increased with extended hydrothermal treatment.

Hydrogen Storage Capacity

The hydrogen adsorption isotherms at 77 K up to 1 bar are shown in Fig. 5. The AC before N doping showed an outstanding hydrogen uptake of 2.74 wt.% at 77 K due to the high S_{BET}(3202 m^2/g) and V_{DR} (1.01 cm^3/g). After the hydrothermal N doping treatment, the NAC samples had hydrogen uptakes of 2.80 wt.%, 2.89 wt.%, and 3.10 wt.%, which were increased with extended hydrothermal time. Therefore, the hydrothermal N doping treatment had a positive effect on the hydrogen storage capacity at 77 K, which was increased by 13%. Figure 6 clearly shows that the hydrogen storage capacities increased linearly with both the S_{BET} and N content.

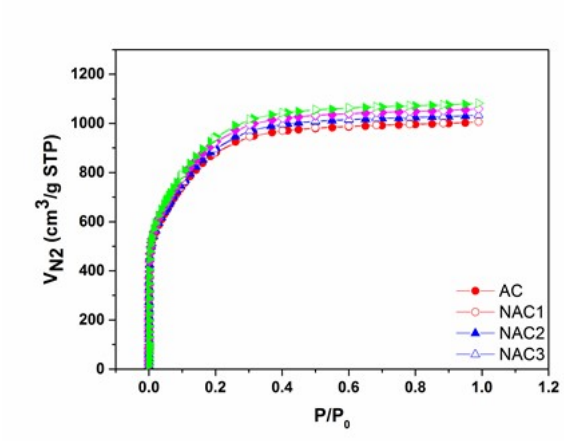

(a)

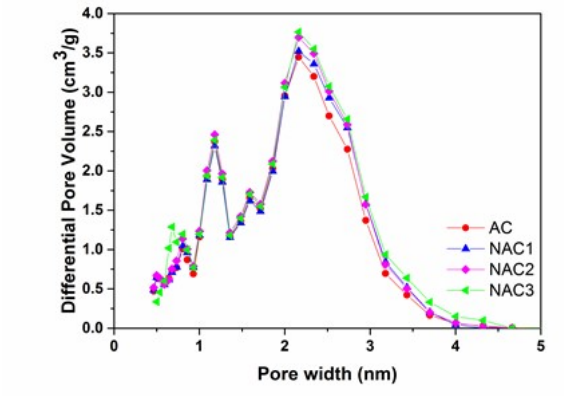

(b)

Fig. 4. N_2 adsorption-desorption isotherms at 77 K (a) and pore-size distributions of all ACs (b)

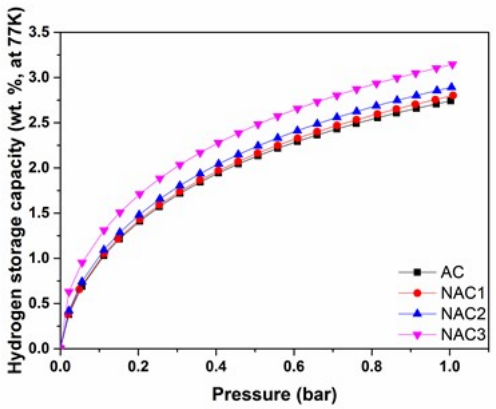

Fig. 5. H_2 adsorption isotherms

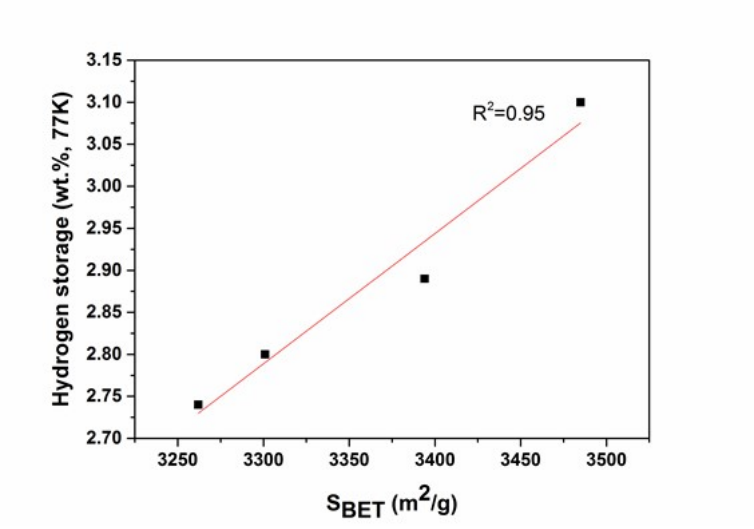

(a)

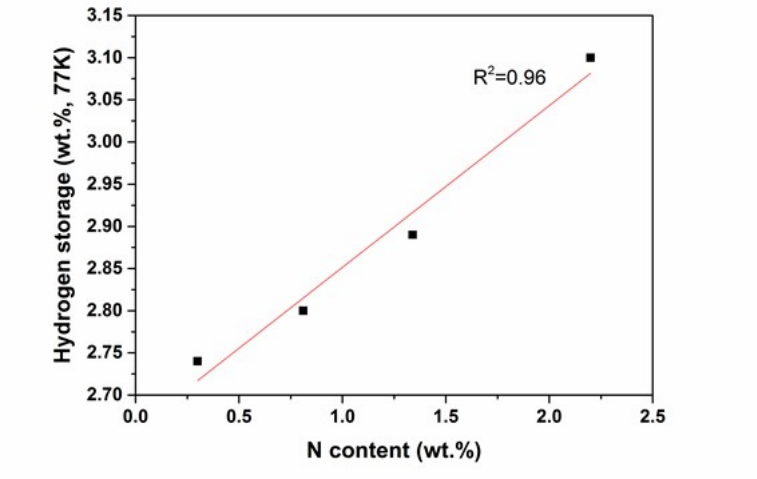

(b)

Fig. 6. The impact of S_{BET} and N content on the hydrogen storage capacity.

Statistical Analysis

Table 2 summarizes the linear model fitting of the experimental data without the constant. The first data column shows the values of the variables considered (N content and surface area) in the model. The second data column shows non-standardized coefficients in the regression equation for predicting the hydrogen storage. The third data column shows the standard errors associated with the

coefficients. Finally, the last two columns are the t (from t-test) and P values. Equation 1 shows the regression equation that best fitted the experimental hydrogen storage capacity.

H_2 uptake = 0.1180 × N content + 0.00082 × BET surface area (1)

Table 2. Statistics of the Linear Model

	B	Std. error	t	P
N content	0.118	0.035	3.325	0.080
Surface area	$8.2*10^{-4}$	$1.43*10^{-5}$	57.225	$3.05*10^{-4}$

Figure 7 demonstrates the prediction of hydrogen storage capacity obtained from Eq. 1. This equation also calculated the contribution of both N content and surface area to the H_2adsorption, as shown in Fig. 8. The results showed that both the N content and surface area had positive contributions to hydrogen storage, and the N doping contributed as much as 8% of hydrogen uptake.

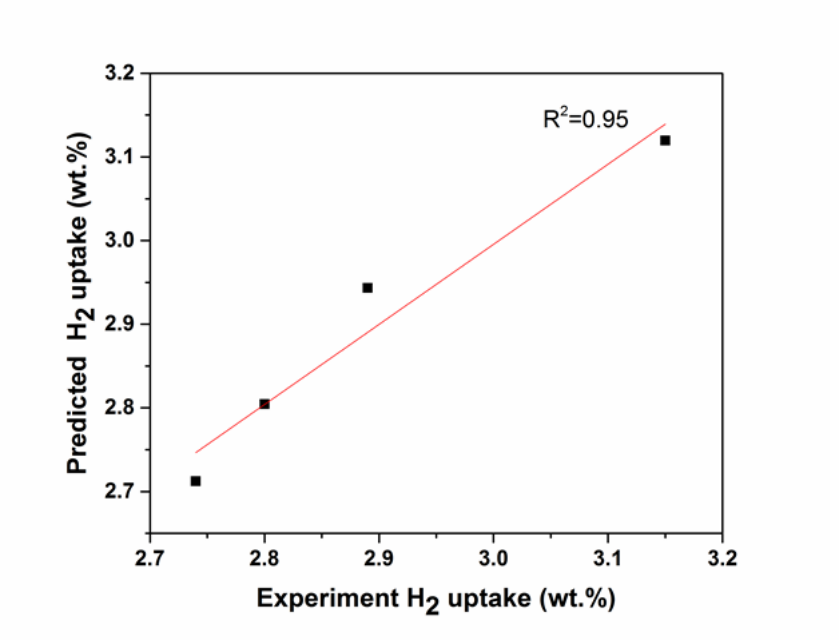

Fig. 7. Correlation between experimental H_2 uptakes and their values predicted from Eq. 1

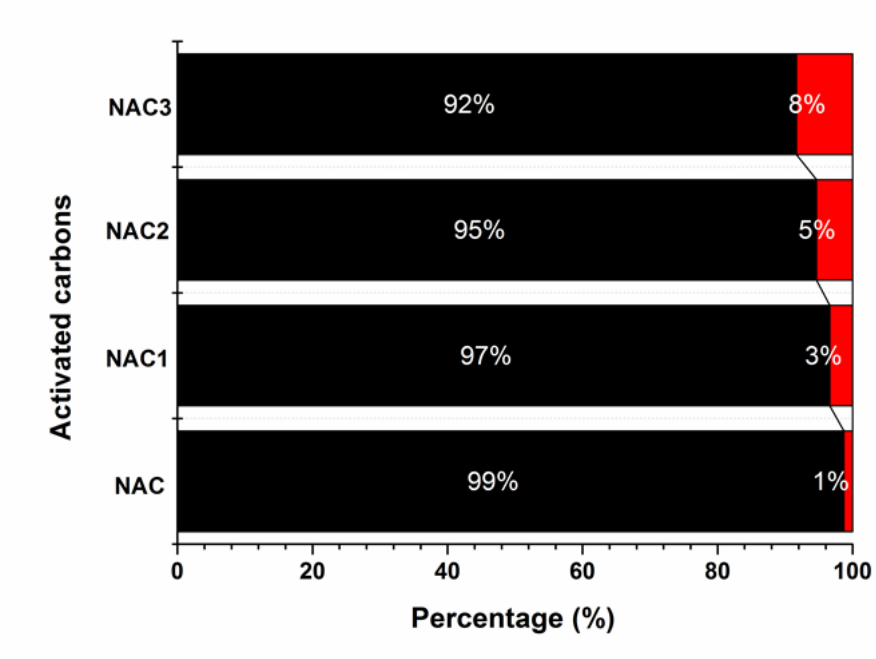

Fig. 8. The contribution of N content (red) and surface area (black) to the H_2 adsorption

Comparison with Literature

The nitrogen doped carbon materials for H_2 storage from different precursors in the literature were compared with the experimental ACs, as summarized in Table 3.

Table 3. Comparison of N-Doped Carbon Materials for H_2 Storage

Carbon Materials	N content (wt.%)	Surface Area (m^2/g)	H_2 Uptake (wt.%)	Ref.
NAC	2.2	3485	3.1	This work
PUF foam	1.50	1674	1.90	Zhao *et al.* 2017
Porous carbon[a]	1.57	1741	1.75	Wang *et al.* 2016
	0.98	2919	2.71	Wang *et al.* 2016
Carbon xerogel	5.48	1357	1.85	Kang *et al.* 2009
Mesoporous nitrogen-doped carbon[a]	N	334	0.53	Zheng *et al.* 2010
	N	2498	2.34	Zheng *et al.* 2010
	N	1810	1.62	Zheng *et al.* 2010
Activated carbon[a]	7.1	2160	2.20	Zhao *et al.* 2013
Porous carbon	18.6	865	1.03	Zhang *et al.* 2015
[a] prepared with KOH activation				

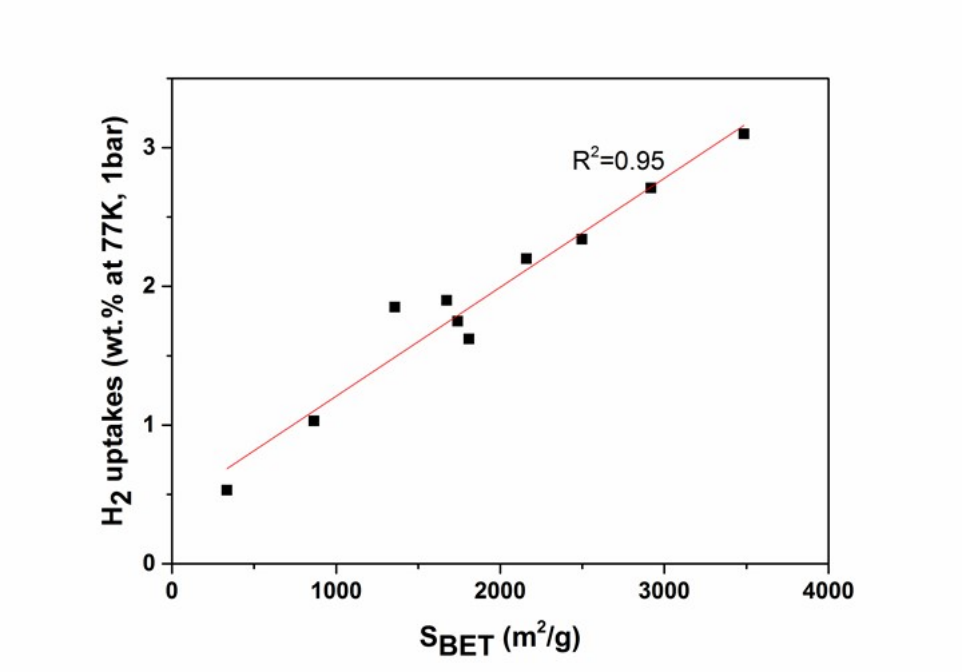

Fig. 9. The impact of surface area on the hydrogen storage at 77 K and 1 bar

As previously mentioned, the pores could be produced into materials by two approaches, which are physical (CO_2 and steam) and chemical (KOH, NaOH, $ZnCl_2$, H_3PO_4) methods. Chemical activation results in a more uniform pore structure and higher carbon yield in the ACs. KOH is one of the most effective activating agents for producing high surface area ACs, which corresponds to the highest hydrogen storage capacity, as shown in Table 3. When the relationship between H_2 storage capacity and the surface area or nitrogen content of all these carbons was examined, the H_2 uptake at 77 K and 1 bar did not have any direct correlation with the N content, but it had a linear relationship with the surface area, as shown in Fig. 9. Thus, it could be concluded that the hydrogen storage capacity of the N-doped carbon materials was determined by the surface area. However, the contribution of N content to the hydrogen storage capacity varied due to the effect of the doping process on the surface area. It was also obvious that the experimental results were among the best in carbon materials for the hydrogen storage.

CONCLUSIONS

1. N-doped microporous activated carbons were obtained by using hydrothermal doping and ammonia as the nitrogen precursor. This was found to be a facile method to successfully obtain N doped high surface area ACs with improved hydrogen storage.
2. The developed N doped ACs with surface areas (S_{BET}) as high as 3485 m^2/g and N content as high as 2.2 % from XPS analysis were achieved. Both the surface area and hydrogen storage capacities were increased due to the hydrothermal doping.
3. The statistical analysis results showed that the hydrogen storage capacities at 77 K and 1 bar could be predicted by the linear model from the N content and surface area. The contribution of the N content can reach up to 8% of total hydrogen storage.
4. The hydrogen uptake was achieved up to 3.1 wt.% at 77 K and 1 bar, which was among the best in carbon materials for hydrogen storage. The hydrogen storage of N-doped carbon material was predominated by the surface area, which could be improved by the hydrothermal doping.

ACKNOWLEDGMENTS

The present research was supported by the National Natural Science Foundation of China (31300488) and Fujian Agriculture and Forestry University Fund for Distinguished Young Scholars (xjq201420).

REFERENCES CITED

Adhikari, A. K., Lin, K. S., and Tu, M. T. (2016). "Hydrogen storage capacity enhancement of mil-53(cr) by pd loaded activated carbon doping," *J. Taiwan Inst. Chem. E.* 63, 463-472. DOI: 10.1016/j.jtice.2016.02.033.

Brunauer, S., Emmet, P. H., and Teller, E. (1938). "Adsorption of gases on multimolecular layers," *J. Am. Chem. Soc.* 60(2), 309-319. DOI: 10.1021/ja01269a023.

Dubinin, M. M., and Polstyanov, E. F. (1989). "Adsorption properties of carbon adsorbents communication 7. Theoretical analysis of the experimental data on the equilibrium adsorption of vapors of substances on activated charcoals with various microporous structures," *Pure. Appl. Chem.* 61(3), 457-467. DOI: 10.1007/BF00849367

Fan, X., Yu, C., Yang, J., Ling, Z., and Qiu, J. (2014). "Hydrothermal synthesis and activation of graphene-incorporated nitrogen-rich carbon composite for high-performance supercapacitors," *Carbon* 70, 130-141. DOI: 10.1016/j.carbon.2013.12.081.

Fu, J., Wang, M., Zhang, C., Zhang, P., and Xu, Q. (2012). "High hydrogen storage capacity of heteroatom-containing porous carbon nanospheres produced from cross-linked polyphosphazene nanospheres," *Mater. Lett.* 81, 215-218. DOI: 10.1016/j.matlet.2012.04.152.

Gregg, S. J., and Sing, K. S. W. (1982). *Adsorption, Surface Area and Porosity* (2nd Ed.), Academic Press, London, UK. DOI: 10.1149/1.2426447.

Huang, H., Hsieh, H., Lin, I., Tong, Y., and Chen, H. (2015). "Hydrogen adsorption and storage in heteroatoms (B, N) modified carbon-based materials decorated with alkali metals: a computational study," *J. Phys. Chem. C.* 119(14), 7662-7669. DOI: 10.1021/acs.jpcc.5b01416.

Hubner, O., Gloss, A., Fichtner, M., and Klopper, W. (2004). "On the interaction of dihydrogen with aromatic systems," *J. Phys. Chem. A.* 108(15), 3019-3023. DOI: 10.1021/jp031102p.

Hwang, S. H., Choi, W. M., and Sang, K. L. (2015). "Hydrogen storage characteristics of carbon fibers derived from rice straw and paper mulberry," *Mater. Lett.* 167, 18-21. DOI: 10.1016/j.matlet.2015.12.118.

Kang, K. Y., Lee, B. I., and Lee, J. S. (2009). "Hydrogen adsorption on nitrogen-doped carbon xerogels," *Carbon* 47(4), 1171-1180. DOI: 10.1016/j.carbon.2009.01.001.

Pietrzak, R., Wachowska, H., and Nowicki, P. (2006). "Preparation of nitrogen-enriched activated carbons from brown coal," *Energ. Fuel.* 20(3), 1275-1280. DOI: 10.1021/ef0504164.

Sari, F. N. I., and Ting, J. (2015). "One step microwaved-assisted hydrothermal synthesis of nitrogen doped graphene for high performance of supercapacitor," *Appl. Surf. Sci.* 355, 419-428. DOI: 10.1016/j.apsusc.2015.07.123.

Stoeckli, F., Slasli, A., Hugi-Cleary, D., and Guillot, A. (2002). "The characterization of microporosity in carbons with molecular sieve effects," *Micropor. Mesopor. Mat.* 51(3), 197-202. DOI: 0.1016/S1387-1811(01)00482-6.

Tarazona, P. (1995). "Solid-fluid transition and interfaces with density functional approaches," *Surf. Sci.* 331-333, 989-994. DOI: 10.1016/0039-6028(95)00170-0.

Wang, Z., Sun, L., Xu, F., Zhou, H., Peng, X., Sun, D., Wang, J., and Yong, D. (2016). "Nitrogen-doped porous carbons with high performance for hydrogen storage," *Int. J. Hydrogen Energ.* 41(20), 8489-8497. DOI: 10.1016/j.ijhydene.2016.03.023.

Wróbel-Iwaniec, I., Díez, N., and Gryglewicz, G. (2015). "Chitosan-based highly activated carbons forhydrogen storage," *Int. J. Hydrogen Energ.* 40(17), 5788-5796. DOI: 10.1016/j.ijhydene.2015.03.034.

Xia, Y., Mokaya, R., Grant, D. M., and Walker, G. S. (2011). "A simplified synthesis of N-doped zeolite-templated carbons, the control of the level of zeolite-like ordering and its effect on hydrogen storage properties," *Carbon* 49(3), 844-853. DOI: 10.1016/j.carbon.2010.10.028.

Xie, H., Shen, Y., Zhou, G., Chen, S., Song, Y., and Ren, J. (2013). "Effect of preparation conditions on the hydrogen storage capacity of activated carbon adsorbents with super-high specific surface areas," *Mater. Chem. Phys.* 141(1), 203-207. DOI: 10.1016/j.matchemphys.2013.04.045.

Zhang, L., Cai, K., Zhang, F., and Yue, Q. (2015). "Adsorption of CO_2 and H_2 on Nitrogen-doped porous carbon from ionic liquid precursor," *Chem. Res. Chinese U.* 31(1), 130-137. DOI: 10.1007/s40242-015-4224-1.

Zhao, Y., Kim, Y. H., Dillon, A. C., Heben, M. J., and Zhang, S. B. (2005). "Hydrogen storage in novel organometallic buckyballs," *Phys. Rev. Lett.* 94(15), 155504. DOI: 10.1103/PhysRevLett.94.155504.

Zhao, W., Fierro, V., Zlotea, C., Aylon, E., Izquierdo, M. T., Latroche, M., and Celzard, A. (2011). "Optimization of activated carbons for hydrogen storage," *Int. J. Hydrogen Energ.* 36(18), 11746-11751. DOI: 10.1016/j.ijhydene.2011.05.181.

Zhao, W., Fierro, V., Fernández-Huerta, N., Izquierdo, M. T., and Celzard, A. (2013). "Hydrogen uptake of high surface area-activated carbons doped with nitrogen," *Int J Hydrogen Energ.* 38(25), 10453-10460. DOI:10.1016/j.ijhydene.2013.06.048.

Zhao, W., Fan, M., Gao, H., and Wang, H. (2016). "Central composite design approach towards optimization of super activated carbons from bamboo for hydrogen storage," *RSC Adv.* 6(52), 46977-46983. DOI: 10.1039/c6ra06326h.

Zhao, W., Luo, L., and Fan, M. (2017). "Preparation and characterization of nitrogen-containing cellular activated carbon for CO_2 and H_2 adsorption," *Nano* 12(1), 65-74. DOI: 10.1142/S1793292017500072.

Zheng, Z., Gao, Q., and Jiang, J. (2010). "High hydrogen uptake capacity of mesoporous nitrogen-doped carbons activated using potassium hydroxide," *Carbon* 48(10), 2968-2973. DOI: 10.1016/j.carbon.2010.04.037.

Article submitted: April 18, 2017; Peer review completed: July 3, 2017; Revised version received and accepted: July 5, 2017; Published: July 13, 2017.

DOI: 10.15376/biores.12.3.6237-6250